Supplementary Information

Atomic-scale insights into electro-steric substitutional chemistry of cerium oxide

Haiwu Zhang, Ivano E. Castelli*, Simone Santucci, Simone Sanna, Nini Pryds, and Vincenzo Esposito*

Department of Energy Conversion and Storage, Technical University of Denmark, Anker Engelunds Vej 411, DK-2800 Kgs. Lyngby, Denmark

*Corresponding authors: Ivano E. Castelli (ivca@dtu.dk), Vincenzo Esposito (vies@dtu.dk)

1. Potential parameters for classical simulations.

Table S1. Interatomic potential parameters for CeO_2. The cutoff of the short-range potential is set at 15 Å.

Buckingham parameters				Shell model parameters	
M-O^{2-}	*A*/eV	*ρ*/Å	*C*/eV Å^6	*Y*/e	*K*/eV Å^{-2}
Ce^{4+}-O^{2-}	1986.83	0.3511	20.40	7.7	291.75
O^{2-}-O^{2-}	22764.3	0.149	27.89	-2.077	27.29

The potential parameters for Ce^{4+}-O^{2-} and O^{2-}-O^{2-} were directly taken from previous work on reduction and oxygen migration in ceria based oxides by G. Balducci *et al*.[1] The potential parameters for Cd^{2+}, Gd^{3+}, Nd^{3+}, Y^{3+}, Ni^{2+}, Yb^{3+} and Lu^{3+} are taken from Ref2, which are derived by Lewis and Catlow by fitting the properties (lattice parameters, elastic constants, dielectric constant, etc) of simple oxides (M_2O, MO, M_2O_3, and MO_2) with the same set of O^{2-}-O^{2-} interaction.[2, 3] The potential parameters for Hf^{4+}-O^{2-} and Zr^{4+}-O^{2-} were also taken from Ref1. Potential parameters for Li^+, K^+, Rb^+, Fe^{2+}, Co^{2+}, Zn^{2+}, Ca^{2+}, Sr^{2+}, Ba^{2+}, Al^{3+}, Sc^{3+}, Si^{4+}, Ge^{4+} and Sn^{4+} were taken from J. R. Tolchard and M. S. Islam's previous work on doping effects in apatite silicate ionic conductors.[4] For Na^+ and Ti^{4+}, the potential parameters were taken from atomistic simulation work on sodium bismuth titanate by H. Zhang *et al*.[5] Potential parameters for other cations were taken from other related works: Mg^{2+}, In^{3+} and La^{3+} from Ref 6; Mn^{2+} from Ref 7; Fe^{3+} from Ref 8; Eu^{3+} and Pr^{3+} from Ref 9. For classical simulations, the valence state of all the cations and oxide ions are specified in the potential parameters. This is different from DFT-based calculations.

2. Lattice parameters

Table S2. Comparison of experimental lattice constant (a, Å) and bond of Ce-O ($d_{Ce\text{-}O}$, Å) of pure CeO_2 with simulated results.

	Exp	Classical Simulations	LDA	GGA	GGA+U
a, Å	5.412,[10] 5.407[11]	5.429	5.546	5.406	5.445
$d_{Ce\text{-}O}$, Å	2.34346,[10] 2.3413[11]	2.35096	2.40149	2.34079	2.3581

3. Full list of defect equations

1) Monovalemt (M^+) cations: $M_2O + 2Ce_{Ce}^{\times} + 3O_O^{\times} \rightarrow 2M_{Ce}^{'''} + 3V_O^{\bullet\bullet} + 2CeO_2$

$$E_{sol,\,mono} = (2E_{CeO_2} + 3E_{def}\left(V_O^{\bullet\bullet}\right) + 2E_{def}\left(M_{Ce}^{'''}\right) - E_{M_2O})/2$$

2) Divalent (M^{2+}) cations: $MO + Ce_{Ce}^{\times} + O_O^{\times} \rightarrow M_{Ce}^{''} + V_O^{\bullet\bullet} + CeO_2$

$$E_{sol,\,div} = E_{CeO_2} + E_{def}\left(V_O^{\bullet\bullet}\right) + E_{def}\left(M_{Ce}^{''}\right) - E_{MO}$$

3) Trivalent (M^{3+}) cations: $M_2O_3 + 2Ce_{Ce}^{\times} + O_O^{\times} \rightarrow 2M_{Ce}^{'} + V_O^{\bullet\bullet} + 2CeO_2$

$$E_{sol,\,tri} = (2E_{CeO_2} + E_{def}(V_O^{\bullet\bullet}) + 2E_{def}(M_{Ce}^{'}) - E_{M_2O_3})/2$$

4) Tetravalent (M^{4+}) cations: $MO_2 + Ce_{Ce}^{\times} \rightarrow M_{Ce}^{\times} + CeO_2$

$$E_{sol,\,tetr} = E_{CeO_2} + E_{def}(M_{Ce}^{\times}) - E_{MO_2}$$

4. Energy profile obtained by classical simulations

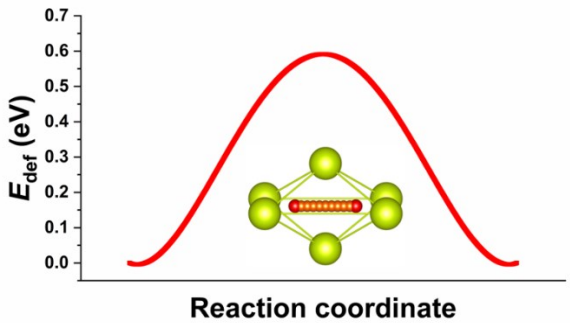

Fig. S1 Defect site energy as a function of reaction coordinate for oxygen ion migration within pure CeO_2 obtained by the MS simulations using GULP. Colors: Ce^{4+}, yellow; oxygen, red.

5. Mean-squared displacements for 'pure' system

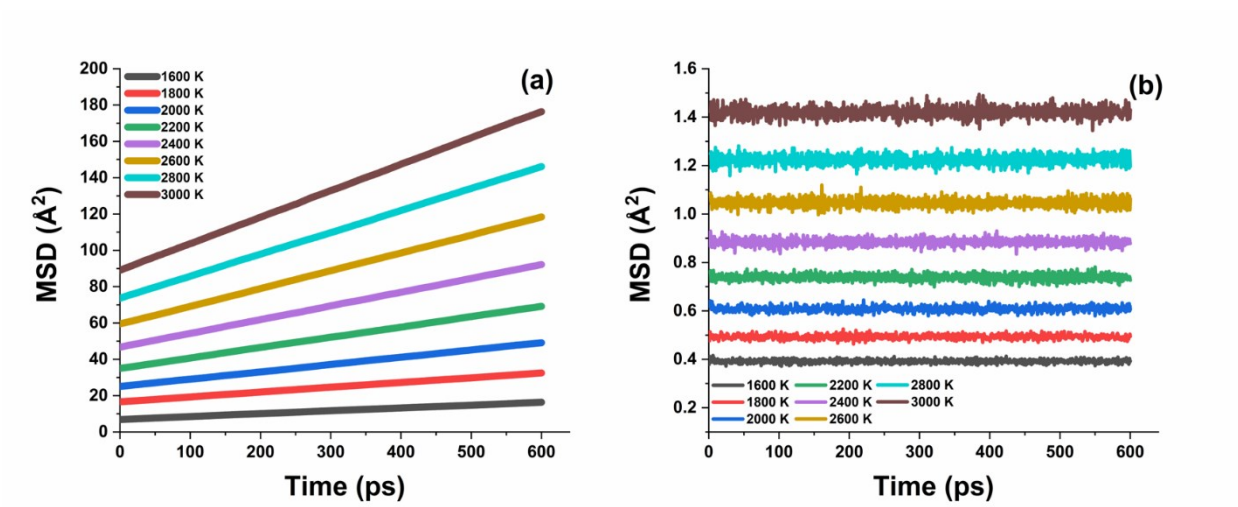

Fig. S2. Temperature dependent MSDs of (a) oxygen ions and (b) Ce^{4+} cations of 'pure' CeO_2. Oxygen ions show significant diffusion. The MSDs for cations converge quickly after equilibrate, indicating that no cation diffusion has taken place in the simulation cells on the simulation time scale.

6. Oxygen ion diffusion in co-substituted systems

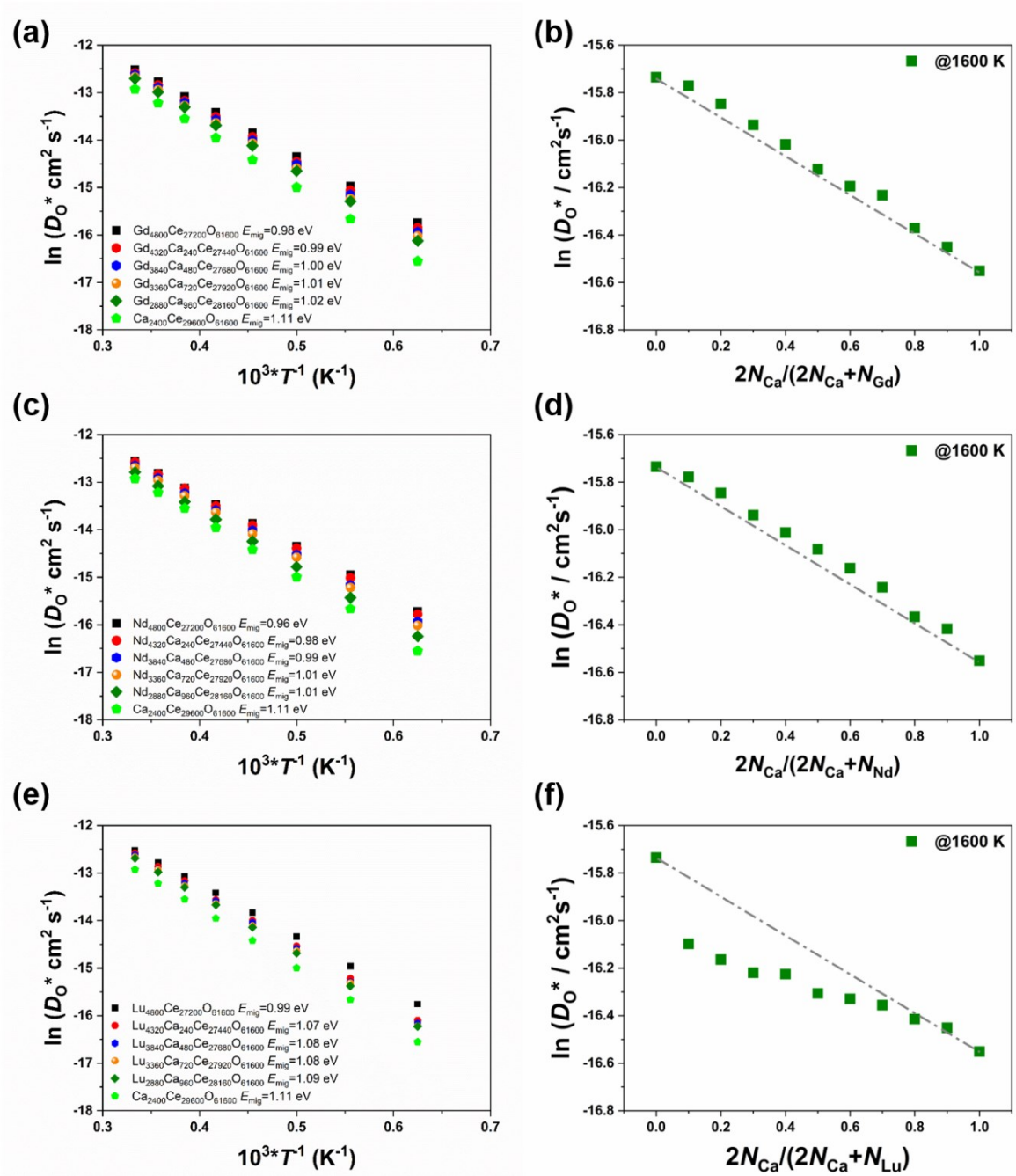

Fig. S3. Inverse temperature dependent oxygen tracer diffusion coefficients (D_O^*) for (a) Gd^{3+}/Ca^{2+}; (c) Nd^{3+}/Ca^{2+}; (e) Lu^{3+}/Ca^{2+} co-substituted systems. Oxygen tracer diffusion coefficients (D_O^*) for (b) Gd^{3+}/Ca^{2+}; (d) Nd^{3+}/Ca^{2+}; (f) Lu^{3+}/Ca^{2+} co-substituted systems as a function of Ca^{2+} concentration (*N* is the number of substituent cations). The lines in (b), (d) and (f) represent the expected D_O^* based on a weighted average. The oxygen vacancy concentration ($x_{V_O^{\bullet\bullet}}$) is 2.5% for all the co-substituted systems.

7. Traced trajectories for various cations substituted systems

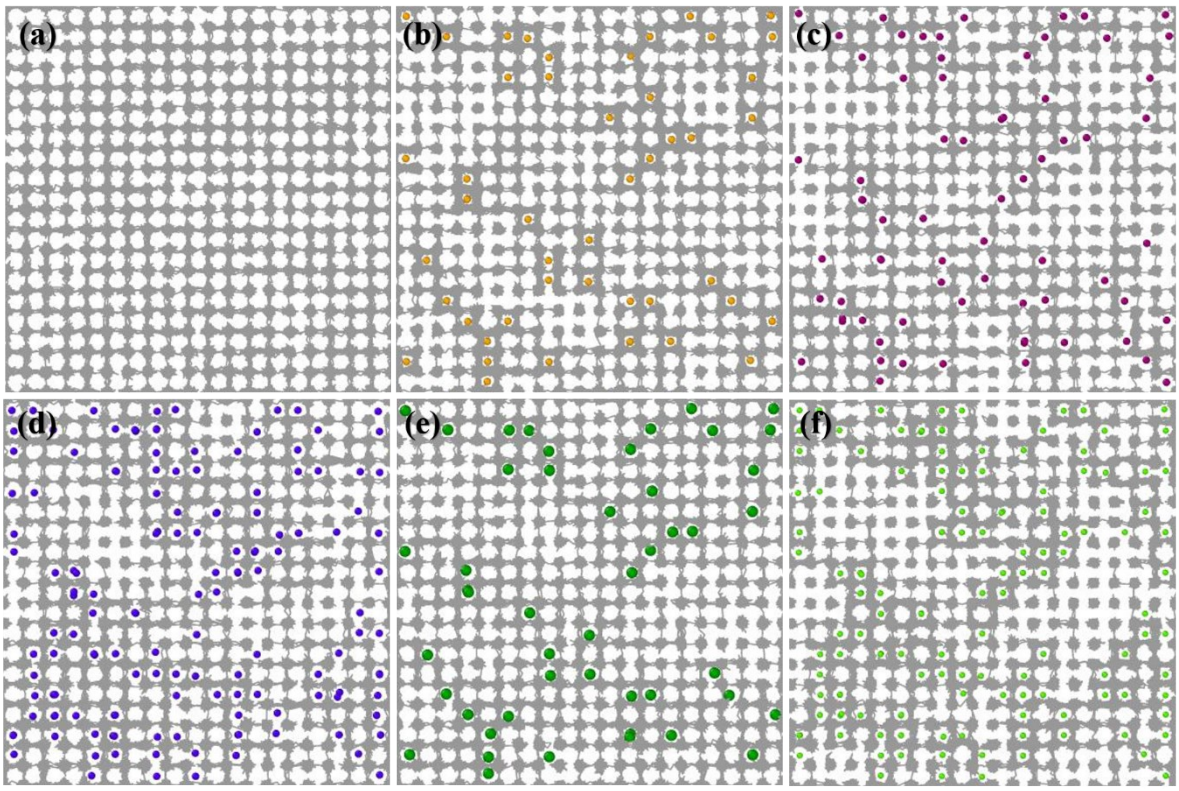

Fig. S4. Traced trajectories for oxygen ion of (a) pure CeO_2; and CeO_2 substituted by (b) Na^+; (c) Ca^{2+}; (d) Gd^{3+}; (e) K^+, and (f) Si^{4+} at *t*=80 ps at 2400 K projected onto the *ab* plane. The Ce^{4+} and O^{2-} ions are omitted for clarify. Note that the radii of the cations does not correspond to the real size. Colors: Na, orange; Ca, purple; Gd, violet; K, olive; Si, green.

8. Oxygen ion migration

Table S3. Energy barrier for blocking (E_{block}, eV) and trapping (E_{trap}, eV) mechanisms for oxide-ion migration with various diffusion pathways. The values for E_{trap} correspond to an oxygen ion jumping from the nearest-neighboring site to the next nearest-neighboring site, whereas the values in the brackets correspond to the reverse process. Energy difference (E_{diff}, eV) of E_{trap} compared to the oxygen ion migration within pure CeO_2.

	K^+	Ni^{2+}	Ba^{2+}	Al^{3+}	K^+/Ca^{2+}*	Ni^{2+}/Ca^{2+}*	Cd^{2+}/Ca^{2+}*	Sr^{2+}/Ca^{2+}*
E_{block}	1.26	0.27	1.57	0.51	1.18	0.21	0.67	1.07
E_{trap}	0.13(0.58)	0(0.97)	0.15(0.36)	0.60(1.18)	0.32(0.55)	0.0(0.81)	0.17(0.78)	0.40(0.54)
E_{diff}	-0.40(0.05)	-0.53(0.44)	-0.38(-0.17)	0.07(0.65)	-0.21(0.02)	0.56(0.25)	-0.36(0.25)	-0.13(0.01)

*Oxygen ion diffusion with a fixed saddle point configuration of $Ca_{Ce}^{''}$

References

1 G. Balducci, M. S. Islam, J. Kaspar, P. Fornasiero, M. Graziani, *Chem. Mater*. 2000, **12**, 677-681.
2 G. V. Lewis, C. R. A. Catlow, *J. Phys. C Solid State Phys*. 1985, **18**, 1149-1161.
3 C. R. A. Catlow, *Proc. R. Soc. Lond. A*. 1977, **353**, 533-561.

4 J. Tolchard, P. R. Slater, M. S. Islam, *Adv. Funct. Mater*. 2007, **17**, 2564-2571.
5 H. Zhang, A. H. H. Ramadan, R. A. De Souza, *J. Mater. Chem. A*. 2018, **6**, 9116-9123.
6 J. M. Clark, S. Nishimura, A. Yamada, M. S. Islam, *Angew. Chem. Int. Ed*. 2012, **51**, 13149-13153
7 M. S. Islam, and C. R. A. Catlow, *J. Phys. Chem. Solids*, 1988, **49**, 119-123
8 M. Cherry, M. S. Islam, and C. R. A. Catlow, *J. Solid. State. Chem*, 1995, **118**, 125-132.
9 M. V. dos S. Rezende, M. E. G. Valerio, R. A. Jackson, *J. Solid. State. Chem*, 2011, **184**, 1903-1908.
10 M. Wolcyrz, L. Kqpinski, *J. Solid State Chem*. 1992, **99**, 409-413.
11 M. Yashima, S. Kobayashi, T. Yasui, *Solid State Ionics*. 2006, **177**, 211-215.